JOURNAL OF Materials CHEMISTRY

2,2′-Bipyridines carrying a diazo moiety and their complexes with bis(hexafluoroacetylacetonato)copper: synthesis, structures, electronic and magnetic properties of their photoproducts in frozen solutions†

Hiroshi Morikawa,[a] Fumika Imamura,[a] Yasuo Tsurukami,[a] Tetsuji Itoh,[a] Harumi Kumada,[a] Satoru Karasawa,[a] Noboru Koga*[a] and Hiizu Iwamura[b]

[a]*Graduate School of Pharmaceutical Sciences, Kyushu University, 3-1-1 Maidashi, Higashi-ku, Fukuoka 812-8582, Japan. E-mail: koga@phar.kyushu-u.ac.jp*
[b]*The University of the Air, 2-11 Wakaba, Mihama-ku, Chiba 261-8586, Japan*

Received 12th September 2000, Accepted 13th November 2000
First published as an Advance Article on the web 10th January 2001

4-(α-Diazobenzyl)-2,2′-bipyridine **2**, diazodi{4-(2,2′-bipyridyl)}methane **3**, and 1,3-benzenediyl{4-(4′-methyl-2,2′-bipyridyl)diazomethane} **4** were prepared as new types of spin sources/magnetic couplers. The molecular structures of bipyridine ligands, **2**, **3**, **4**, and [Cu(hfac)$_2$·**2**] were revealed by X-ray analyses. Photolysis of **2**, **3**, **4**, and their complexes with Cu(hfac)$_2$ in MTHF frozen solutions at cryogenic temperature was followed by UV–Vis and EPR spectroscopy. UV–Vis and EPR spectra after photolysis showed strong two absorptions; at 508 and 471 nm for **2**, and 511 and 476 nm for **3**, and characteristic sets of EPR signals due to the triplet states; $|D/hc| = 0.418$, and 0.436 cm^{-1} and $|E/hc| = 0.021$ and 0.022 cm^{-1} for **2** and **3**, respectively. Diazo compound **4** after photolysis also showed absorptions at 506 and 471 nm and EPR signals characteristic of a quintet. Their complexes with Cu(hfac)$_2$ showed a red shift of 3–14 nm in the visible spectra and gave EPR spectra characteristic of the high-spin complexes under similar conditions. Magnetic susceptibility measurements on a SQUID magnetometer were carried out using a sample similar to the one employed in the UV–Vis and EPR studies. The field dependence of magnetization in frozen solution suggested that the ground-state spin multiplicities of the photoproducts of **2**, **3**, and **4** were triplet, triplet, and quintet, respectively. Similarly, those of their complexes with Cu(hfac)$_2$ were quartet, quintet, and septet, respectively.

Introduction

Heterospin systems consisting of 2p spins of diarylcarbenes and 3d spins of transition metal ions have been employed in our laboratories for the construction of photoresponsive super-high-spin complexes.[1] Photolysis of 1 : 1 polymeric complexes of bis(hexafluoroacetylacetonato)-manganese(II) and -copper(II), {Mn(hfac)$_2$ and Cu(hfac)$_2$}, coordinated with diazodi(4-pyridyl)methane **1** indeed produced ferri- and ferromagnetic chains with average spins of approximately $S = 300$ (at 1.9 K) and 30 (3.0 K), respectively.[2,3] Since the obtained metal complexes with **1** were basically one-dimensional, spontaneous magnetization was not obtained at finite temperature. These studies revealed the usefulness of the heterospin complexes and, at the same time, the necessity of a two- or three-dimensional (2D and 3D) structure for the realization of molecule-based magnets.[4] One approach to the construction of 2D or 3D structures in our heterospin systems lies in the use of a metal ion with only one type of ligand, such as hfac. The bidentate ligand 2,2′-bipyridine is a candidate[5] for such a base ligand; 2,2′-bipyridine is well known to produce bis and tris complexes coordinated with various central metal ions.[6] For this purpose, diazodi{4-(2,2′-bipyridyl)}methane **3** and 1,3-benzenediyl{4-(4′-methyl-2,2′-bipyridyl)diazomethane} **4** were designed and prepared as new photoresponsive spin precursor/magnetic couplers. Compounds **3** and **4** are bis-bidentate ligands so that they could lead to complexes having extended structures by coordinating with metal ions. 4-(α-Diazobenzyl)-2,2′-bipyridine **2** was also prepared as a reference compound. In the first step, the complexes of Cu(hfac)$_2$ coordinated with **2**, **3**, and **4** were photolysed and their electronic and magnetic properties were investigated. The electronic and magnetic data are important in understanding magnetic couplings between generated carbene(s) and copper(II) ion(s) through 2,2′-bipyridine rings. In the previous work, we employed crystalline samples for photolysis and often encountered problems associated with the optical transparency of the samples. To overcome these difficulties, it was deemed necessary to develop studies in frozen solution systems for the SQUID measurements and confirm the ground-state spin multiplicity.[7] In frozen solution, two new factors have to be taken into account. One is dissociation of the metal complexes; generally high association constants of 2,2′-bipyridine ligands will be favorable in this respect. Secondly, a small amount of paramagnetic species and a large amount of diamagnetic solvent molecules are present in the sample and they compete with each other magnetically. In particular, it is difficult to estimate the diamagnetic contribution accurately in a sample for paramagnetic species with a small S value. A problem for magnetic experiments in frozen solution lies in how accurately the diamagnetic contribution of the solvent in a sample is estimated. In our diazo-carbene system, however, this problem can be resolved by using the difference between the magnetization values (M) before and after irradiation without touching the sample in between. An additional advantage of frozen solution conditions is that we may neglect intermolecular antiferromagnetic interactions which are often observed at low

†Electronic supplementary information (ESI) available: EPR spectra after irradiation of **2**, **3**, **4**; M/M_{sat} *vs.* H/T plots after irradiation of **3** in frozen solutions of MTHF. See http://www.rsc.org/suppdata/jm/b0/b007375j/

temperatures (<10 K) in a crystalline sample. In this paper, we report SQUID measurements under frozen 2-methyltetrahydrofuran (MTHF) solutions (similar to those for UV–Vis and EPR studies) and the determination of the ground state spin multiplicity for [(Cu(hfac)$_2$)$_2$·**3**] and [(Cu(hfac)$_2$)$_2$·**4**]. According to previous studies[8] of the copper complexes with 4-*tert*-butylaminoxyl-2,2′-bipyridine **5**, high-spin copper complexes with $S=4/2$ and 6/2 are expected to be produced after photolysis of [(Cu(hfac)$_2$)$_2$·**3**] and [(Cu(hfac)$_2$)$_2$·**4**], respectively.

Results and discussion

Preparation of diazo-bipyridines and their copper complexes

4-Bromo-2,2′-bipyridine[9] and 4-methyl-4′-formyl-2,2′-bipyridine were used as starting materials for **3** and **4**, respectively. The bromide **3′Br** was lithiated, reacted with 2-bromo-4-formylpyridine, followed by oxidation with MnO_2. The obtained bipyridyl pyridyl ketone **3′k** was reacted with 2-trimethylstannylpyridine in the presence of $Pd(PPh_3)_4$ to give bis(4-(2,2′-bipyridyl)) ketone **3k**. The diketone **4k** was prepared by the reaction of 4-methyl-4′-formyl-2,2′-bipyridine with the dilithiated salt of 1,3-dibromobenzene, followed by oxidation with MnO_2. The diazo groups that are precursors to the carbenes were synthesized from the corresponding carbonyl groups *via* hydrazones using a standard procedure.[2] The preparations of diazo-bipyridines **3** and **4** are summarized in Scheme 1. A reference diazo compound **2** was prepared in a manner similar to the procedure for **1** using 4-benzoyl-2,2′-bipyridine in place of di(4-pyridyl) ketone.[1]

After recrystallization from *n*-hexane/ether (1 : 1), MeOH/CH_2Cl_2/ether (2 : 1 : 1), and CH_2Cl_2/*n*-hexane (10 : 1), bipyridine ligands **2**, **3**, and **4** were obtained as red needles, orange plates, and red plates, respectively.

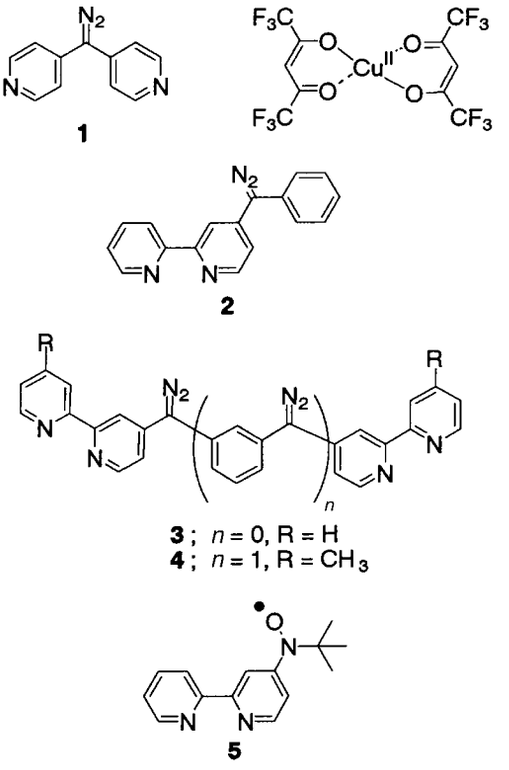

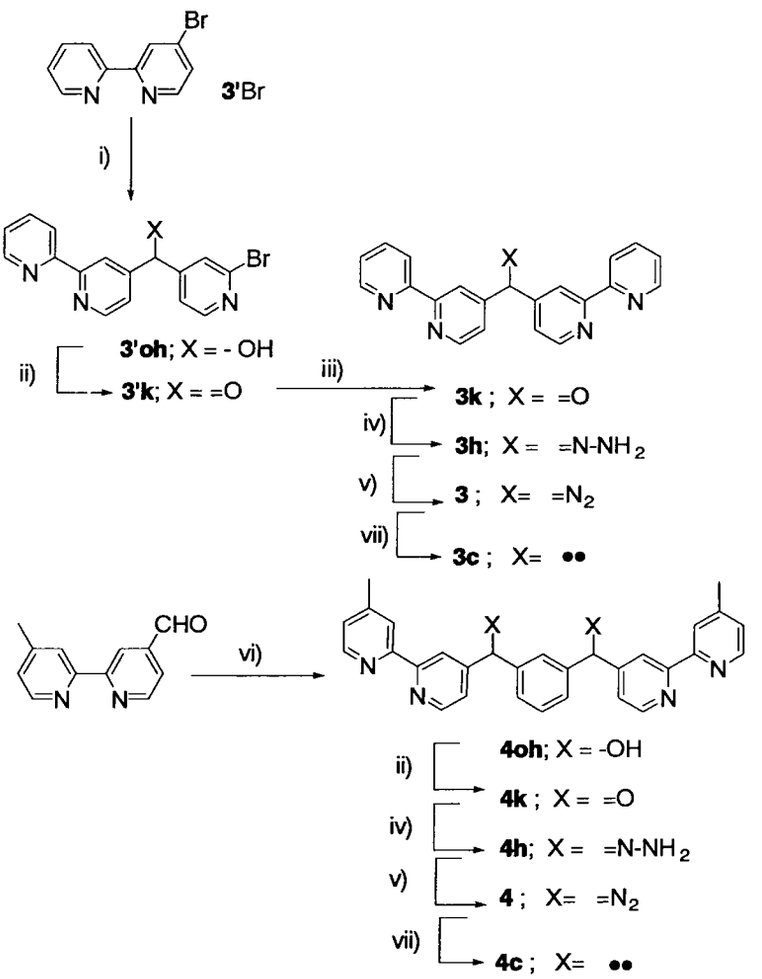

Scheme 1 i) 2-Bromo-4-formylpyridine, *n*-BuLi/ether, −78 °C; ii) MnO_2/$CHCl_3$, reflux; iii) 2-trimethylstannylpyridine, $Pd(PPh_3)_4$/toluene, reflux; iv) NH_2NH_2, NH_2NH_2·HCl/DMSO; v) MnO_2/CH_2Cl_2; vi) 1,3-dibromobenzene, *n*-BuLi/THF, −78 °C; vii) *hν*.

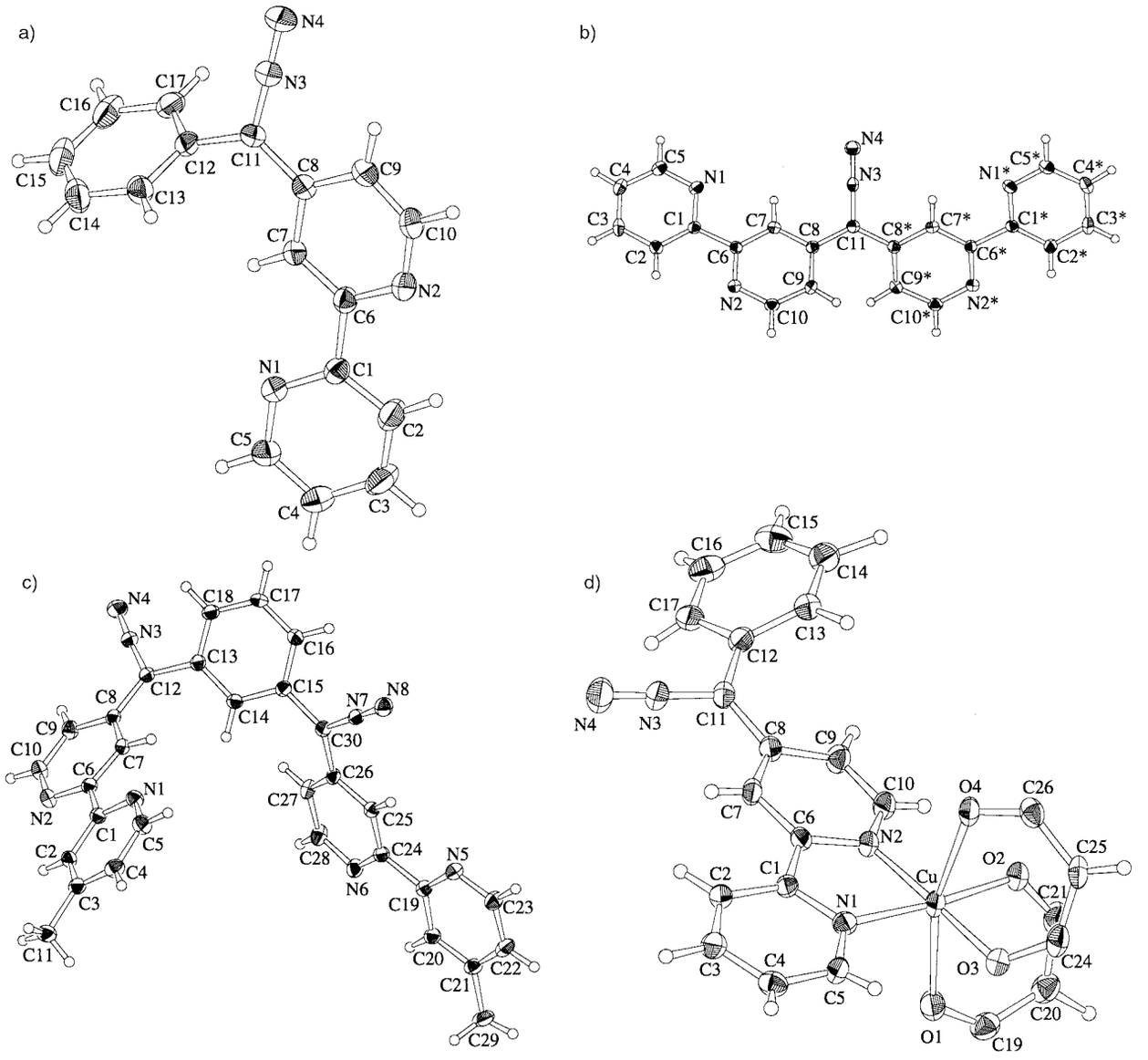

Fig. 1 ORTEP drawings of molecular structures for (a) **2**, (b) **3**, (c) **4**, and (d) [Cu(hfac)$_2$·**2**] with thermal ellipsoid plot at the 30% probability level.

The copper complexes [(Cu(hfac)$_2$)$_2$·**2**], [(Cu(hfac)$_2$)$_2$·**3**], and [(Cu(hfac)$_2$)$_2$·**4**] were prepared by mixing the solutions of **2**, **3**, and **4** with that of Cu(hfac)$_2$ in MTHF in the appropriate ratios. After recrystallization, the complex of [Cu(hfac)$_2$·**2**] was obtained as single crystals and the 2 : 1 complexes, [(Cu(hfac)$_2$)$_2$·**3**], and [(Cu(hfac)$_2$)$_2$·**4**], were obtained as powders.

Characteristic IR absorptions due to the diazo moieties at 2049 cm^{-1} for **2**, **3**, and **4** shifted to 2061, 2074, and 2064 cm^{-1}, respectively, after the complexation with Cu(hfac)$_2$.

Molecular structures of 2, 3, 4, and [Cu(hfac)$_2$·2]

The molecular and crystal structures of the diazo-bipyridines **2**, **3**, and **4**, and the copper complex [Cu(hfac)$_2$·**2**] were revealed

Table 1 Selected bond lengths, angles and dihedral angles for **2**, **3**, **4**, and [Cu(hfac)$_2$·**2**]

	Bond length/Å		Bond angle/°		Dihedral angle/°	
2			C8–C11–C12	127.76	N1C2C4–N2C7C9	14.87
					N2C7C9–C13C15C17	59.36
3			C8–C11–C8*	127.29	N1C2C4–N2C7C9	2.95
					N2C7C9–N2*C7*C9*	50.28
4			C8–C12–C13	128.24	N1C2C4–N2C7C9	8.74
			C15–C30–C26	129.92	N5C20C22–N6C25C27	9.69
					N2C7C9–C14C16C18	51.85
					N6C25C27–C14C16C18	38.74
[Cu(hfac)$_2$·**2**]	Cu–N1	1.999(4)	N1–Cu–O2	173.1(2)	N1C2C4–N2C7C9	8.59
	Cu–N2	1.983(4)	N2–Cu–O3	174.7(2)	N2C7C9–C13C15C17	36.46
	Cu–O1	2.232(4)	O1–Cu–O4	163.2(1)		
	Cu–O2	1.960(4)				
	Cu–O3	1.994(4)	C8–C11–C12	128.03		
	Cu–O4	2.385(4)				

by X-ray analyses. The molecular structures of **2**, **3**, **4**, and [Cu(hfac)$_2$·**2**] are shown in Fig. 1.

Selected bond lengths, angles, and dihedral angles for **2**, **3**, **4**, and [Cu(hfac)$_2$·**2**] are given in Table 1.

The molecular structures of the bipyridine ligands **2** and **4** have no symmetry axis and **3** has a C_2 symmetry axis through the C(11)–N(3)–N(4) bond. As shown in Fig. 1, the 2,2′-bipyridine units in **2**, **3**, and **4** have *trans* conformations[10] and the dihedral angles between the pyridine planes of the bipyridine moiety are 14.87, 2.95, and 8.74(9.69°), respectively. The bond angles of C(8)–C(11)–C(12) in **2**, C(8)–C(11)–C(8*) in **3** and C(8)–C(12)–C(13) (C(15)–C(30)–C(26)) in **4** are 127.76, 127.29, and 128.24(129.92)°, respectively. The dihedral angles between the pyridine ring of bipyridine and phenyl rings for **2** and **4**, and that between the pyridine rings for **3** through the diazo moiety, are 59.36, 51.85 and 38.74, and 50.28°, respectively.

The crystal of [Cu(hfac)$_2$·**2**] contained four molecules of acetone per unit cell as solvent of recrystallization. The molecular structure of the complex [Cu(hfac)$_2$·**2**] has no symmetry axis and the coordination geometry is a distorted octahedron. As listed in Table 1, the elongation axis for [Cu(hfac)$_2$·**2**] is through O(1)–Cu–O(4). Therefore, the magnetic orbital ($d_{x^2-y^2}$) of the copper ion is judged to be directed to the nitrogens (N1 and N2) of the bipyridine in the complex. The dihedral angle between the two pyridine rings in the 2,2′-bipyridine moiety is 8.59° and the one between the planes of the bipyridine and the phenyl ring is 36.46°. The crystal packing showed the head-to-tail dimer structures consisting of a pair of Δ and Λ isomers (the nearest contacts are 3.19 Å for O(1)–C(17) within the dimers and 3.25 Å for O(4)–C(2) between the dimers). This dimer structure was similar to that for the corresponding [Cu(hfac)$_2$·**5**] reported previously.[8]

UV–Vis, EPR spectra and SQUID measurements in frozen solutions

Solutions of the bipyridine ligands **2**, **3**, **4**, and mixed solutions of bipyridines and Cu(hfac)$_2$ in MTHF were used for the sample. They were placed in the cryostats of low-temperature EPR and UV–Vis spectrometers and in the SQUID magnetometer/susceptometer sample room. The sample was irradiated with light of $\lambda > 380$ nm through a colored glass filter from a high-pressure Hg lamp for EPR and UV–Vis experiments and the light from an argon laser ($\lambda = 514$ nm) and or a He–Cd laser ($\lambda = 442$ nm) for SQUID measurements. Selected spectroscopic data ($\nu_{C=N_2}$/cm^{-1} and λ_{max}/nm) and zero-field splitting parameters (zfs) obtained from EPR spectra are summarized in Table 2 together with the data for compound **1** and its Cu(hfac)$_2$ complex.

Table 2 Selected spectroscopic data for the pyridines and their copper complexes

	IR[a]	UV–Vis	EPR	
	$\nu_{C=N_2}$/cm^{-1}	λ_{max}/nm	$\lvert D/hc\rvert$/cm^{-1}	$\lvert E/hc\rvert$/cm^{-1}
1	2060[b]	484, 304[b]		
1c		453, 421	0.434[b]	0.020[b]
[Cu(hfac)$_2$·**1**]	2072			
[Cu(hfac)$_2$·**1c**]				
2	2049	500, 283[c]		
2c		508, 471	0.418	0.021
[Cu(hfac)$_2$·**2**]	2061	360, 295[c]		
[Cu(hfac)$_2$·**2c**]		522, 488, 378		
3	2049	477, 285[c]		
3c		511, 476	0.436	0.022
[(Cu(hfac)$_2$)$_2$·**3**]	2074	355, 291[c]		
[(Cu(hfac)$_2$)$_2$·**3c**]		514, 477		
4	2049	493, 285[c]		
4c		506, 471		
[(Cu(hfac)$_2$)$_2$·**4**]	2064	353, 293[c]		
[(Cu(hfac)$_2$)$_2$·**4c**]		513, 477		

[a]In KBr pellets. [b]Ref. 14. [c]At room temperature.

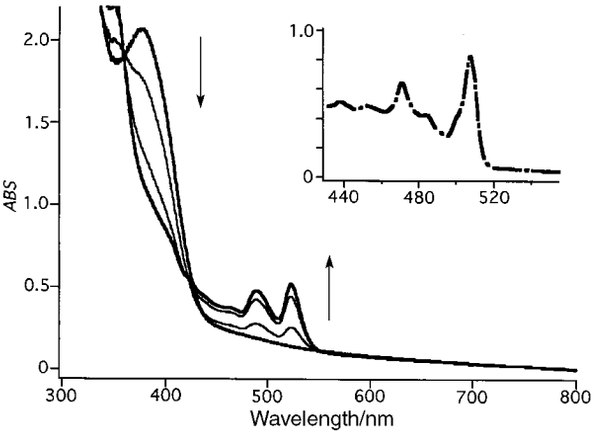

Fig. 2 Change of UV–Vis spectra after irradiation ($\lambda > 380$ nm) of [Cu(hfac)$_2$·**2**] for 0, 10, 20, and 80 s in MTHF frozen solution (1.0×10^{-3} M) at 10 K. The final spectrum of **2** (—·—) is shown in the inset.

(A) UV–Vis spectra of 2, 3, 4 and their complexes with Cu(hfac)$_2$. UV–Vis spectra for diazo-bipyridine **2** in MTHF solution (1 mM) at room temperature showed two absorptions at 283 and 500 nm. The latter is characteristic of the n–π* transition due to the diazo group. When the irradiation ($\lambda > 380$ nm) started at 10 K, this absorption decreased and two new absorptions appeared at 508 and 471 nm. Similarly, diazo-bipyridines **3** and **4** had absorptions at 477 and 493 nm due to the n–π^* transition and exhibited absorptions at 511 and 476, and 506 and 471 nm, respectively, after irradiation under similar conditions. Although the value of λ_{max} showed a red shift of *ca.* 40 nm, the spectra after irradiation of **2**, **3**, and **4** closely resembled that for diphenylcarbene (465 nm) reported previously.[11]

The complexation of Cu(hfac)$_2$ with **2** in MTHF was confirmed by titration by means of UV–Vis absorption (360 nm) at room temperature. The binding constant (log K) for **2** was thus estimated to be 5.8 M^{-1} which is smaller that for 2,2′-bipyridine with Cu(II)(NO$_3$)$_2$ (log $K = 7.92$ M^{-1} at 30 °C in H$_2$O–EtOH) reported previously.[12] The 2 : 1 complexes of Cu(hfac)$_2$ with **3** and **4** showed strong absorptions at 291 and 293 nm together with a new shoulder at 355 and 353 nm, respectively.

The change of the UV–Vis spectrum of [Cu(hfac)$_2$·**2**] in frozen MTHF after irradiation at 10 K is shown in Fig. 2 in addition to the spectrum after complete photolysis of **2** under similar conditions (inset in Fig. 2). The absorption at 378 nm due to [Cu(hfac)$_2$·**2**] decreased with the irradiation time and was replaced with new ones at 522 and 488 nm with isosbestic points at 360 and 420 nm (Fig. 2).

The 2 : 1 complexes of Cu(hfac)$_2$ with **3** and **4** in MTHF frozen solutions were also measured under similar conditions. They gave UV–Vis spectra similar to that from [Cu(hfac)$_2$·**2**]; 514 and 477 nm from [(Cu(hfac)$_2$)$_2$·**3**], and 513 and 477 nm from [(Cu(hfac)$_2$)$_2$·**4**]. As listed in Table 2, characteristic absorptions due to the carbene species in the visible region showed a red shift of 3–14 nm after complexation with Cu(hfac)$_2$.

In these 2,2′-bipyridine derivatives and their complexes with Cu(hfac)$_2$, the absorptions at *ca.* 500 nm due to the generated carbene widely overlapped with those of the diazo moieties; the absorption of the carbenes was over ten times larger than that for the diazo moieties ($\varepsilon = \sim 100$ for **2**). These strong

absorptions due to the generated carbenes might prevent the effective photolysis of starting diazo moieties.

All new absorptions observed after irradiation of **2**, **3**, **4**, and their complexes of $Cu(hfac)_2$ disappeared at temperatures higher than 60 K.

(B) EPR spectra of 2, 3, 4 and their complexes with $Cu(hfac)_2$. The EPR spectra after irradiation of **2**, **3**, and **4** and their copper complexes in frozen MTHF solutions were measured at cryogenic temperatures.

When the irradiation for **2**, **3**, and **4** started at 10 K, new signals appeared. Those for **2** and **3** constituted typical sets of signals due to triplet carbenes[13,14] with zero-field splitting parameters (zfs) $|D/hc| = 0.418$ and $0.436\ cm^{-1}$ and $|E/hc| = 0.021$ and $0.022\ cm^{-1}$, respectively. Interestingly, these zfs values are good agreement with those for the corresponding pyridyl carbenes; $|D/hc| = 0.418$ and $0.434\ cm^{-1}$ and $|E/hc| = 0.021$ and $0.020\ cm^{-1}$ for phenyl pyridyl carbene[13] and dipyridyl carbene,[14] respectively, under similar conditions. This agreement suggested that the degrees of delocalization of the 2pπ spin of the carbene center in 2,2′-bipyridines are similar to those for pyridines and the magnitude of the magnetic coupling similar to $[Cu(hfac)_2 \cdot \mathbf{1}]^2$, $J/k_B = 67$ K, is expected to depend on the copper(II). Bisdiazo compound **4** also showed a typical quintet spectrum ($|D/hc| = ca.$ 0.06–$0.13\ cm^{-1}$)[15] having characteristic signals at around 280 and 400 mT, which resemble that after photolysis of 1,3-benzenediylbis(α-diazobenzyl).

On the other hand, the EPR spectrum after irradiation of the solution of **2** and $Cu(hfac)_2$ in a ratio of 1 : 1 under similar conditions showed a drastic change. When irradiated, a set of new signals appeared in the field range 0–600 mT at the expense of signals at 269, 285, 301, and 322 mT due to copper(II) in $[Cu(hfac)_2 \cdot \mathbf{2}]$. They were more complicated than those expected for an unoriented sample of a quartet molecule.[16]

Mixed solutions of $Cu(hfac)_2$ with **3** and **4** in MTHF were also measured under similar conditions. When the solutions of $Cu(hfac)_2$ with **3** in 1 : 1 and 2 : 1 ratios were irradiated, EPR spectra similar to that for $[Cu(hfac)_2 \cdot \mathbf{2}]$ with a strong signal at 254 mT and two broad ones at 100 and 450 mT were obtained, respectively. In the spectrum after irradiation of the 1 : 2 complex of $Cu(hfac)_2$ with **4**, a strong signal at 83 and a broad one at 293 mT appeared at the expense of the signals at $g = 2$ due to isolated Cu(II) ion in $Cu(hfac)_2$ units. EPR spectra after photolysis of the complexes of $Cu(hfac)_2$ with **2**, **3**, and **4** in frozen MTHF are shown in Fig. 3.

In the observed spectra for all copper complexes, a significant number of signals due to metal-free carbene were not observed, indicating that the 2,2′-bipyridine moiety binds with $Cu(hfac)_2$ quantitatively under these cryogenic conditions.

As the temperature was increased from 10 K, the intensity of all new signals linearly decreased according to the Curie law and all signals disappeared at temperatures higher than 60 K. The observed temperature dependence of the signal intensity suggests that the signals were due to the species in the ground state.

(C) SQUID Measurements of 2, 3, 4 and their complexes with $Cu(hfac)_2$. Magnetization data (M_b and M_a) before and after irradiation of **2**, **3**, **4**, and their copper complexes in frozen MTHF solutions, were obtained at 2.0, 3.0, and 5.0 K in the field range 0–50 kOe. Taking the UV–Vis spectral characteristics into account, we employed an argon ion laser ($\lambda = 514$ nm) and a He–Cd laser ($\lambda = 442$ nm) for the irradiation of the diazo compounds and the copper complexes, respectively, in the SQUID experiments.

*(C)-1 2,2′-Bipyridine ligand, **2**, **3**, and **4**.* The solutions (1.0 mM) of **2**, **3**, and **4** in MTHF were used as the samples for SQUID measurements. The development of magnetization at

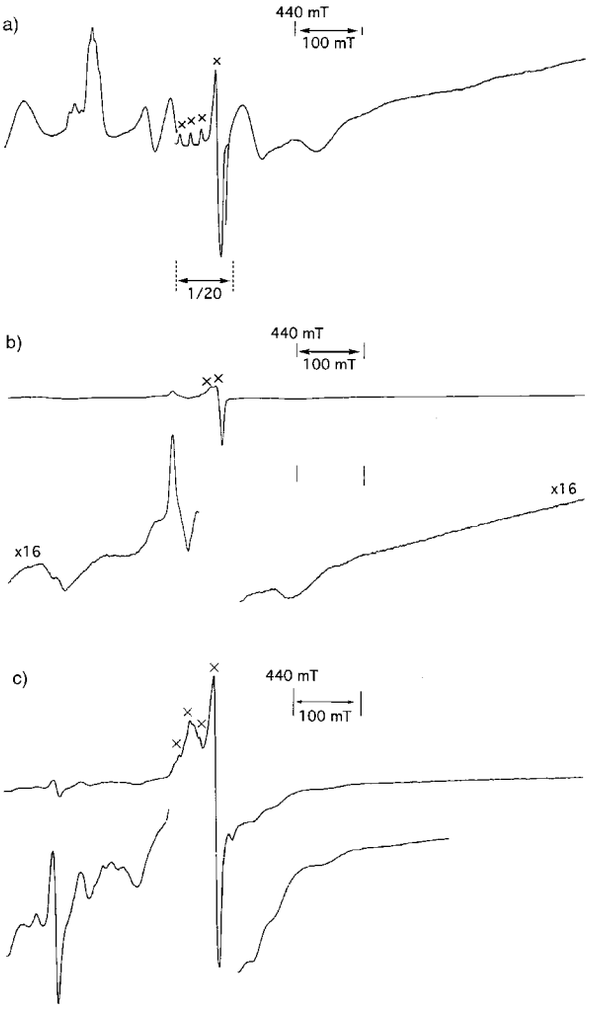

Fig. 3 X-Band ($\nu_0 = 9.45$ GHz) EPR spectra after irradiation ($\lambda > 380$ nm) of the solution (1.0×10^{-3} M) of the complexes of $Cu(hfac)_2$ with (a) **2**, (b) **3**, and (c) **4** in MTHF at 8 K. × indicates the signals due to copper(II) ions of unphotolyzed $Cu(hfac)_2$ units.

5 K in a constant field of 20 kOe with irradiation time for **2** is shown in Fig. 4a. As irradiation was continued, M values gradually increased and reached a plateau after 150 min. The field dependences of the magnetization at 2, 3, and 5 K before and after irradiation (M_a and M_b, respectively) for **2** are given in Fig. 4b. The observed M *vs.* H profile was affected by a large diamagnetic contribution due to the solvent. The magnetization (M) due to the paramagnetic species generated by photolysis was obtained as the difference between M_a and M_b: $M = FM_a - M_b$. The difference of the magnetization before and after irradiation is expressed as follows:

$$M = FM_a - M_b = FNg\mu_B SB(x) \quad (1)$$

where $x = gS\mu_B H/(k_B T)$, F stands for a photolysis factor and the other symbols have their usual meaning. Eqn. (1) fitted experimental data (M *vs.* H/T) to give $S = 1.00 \pm 0.01$ and $F = 0.89 \pm 0.01$ for **2**, $S = 0.99 \pm 0.01$ and $F = 0.88 \pm 0.01$ for **3**, and $S = 1.93 \pm 0.01$ and $F = 0.63 \pm 0.01$ for **4**. Field dependences of M for **2** and **4** are demonstrated *via* the M/M_s *vs.* H/T plots in Fig. 4c together with theoretical curves with $S = 1/2$, 2/2, 3/2, 4/2, and 5/2 in which the M_s values obtained from the best-fitted curves were used. As shown in Fig. 4c, the experimental data for **2c** and **4c** exactly traced the theoretical curves with $S = 2/2$ and 4/2, respectively, indicating that they are triplet and quintet ground states, respectively. Similarly, the experimental data for **3c** indicated a triplet ground state.

From the difference of the absorptions due to diazo moieties in

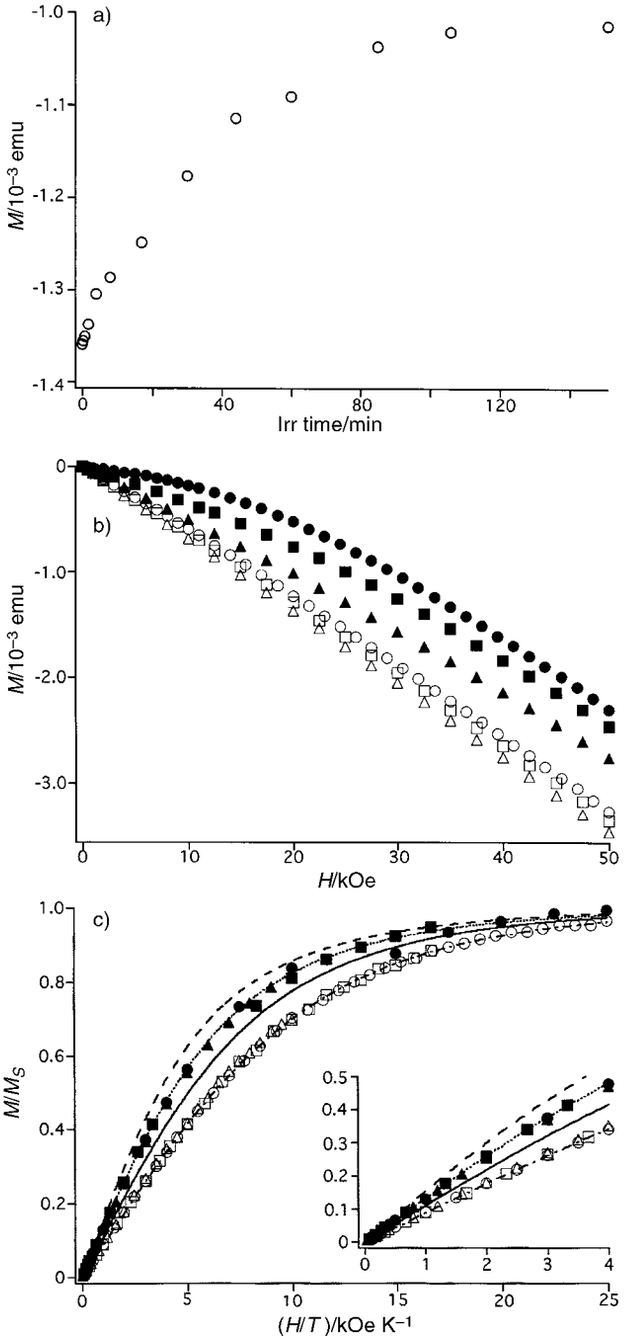

Fig. 4 (a) *M vs.* irradiation time plot for **2** in a constant field of 20 kOe at 5 K. (b) Field dependences of magnetization for **2** at 2.0 (○), 3.0 (□), and 5.0 K (△) before (open) and after (filled) irradiation ($\lambda = 514$ nm) of **2** in MTHF frozen solution. (c) M/M_s *vs.* H/T plot for **2** (open) and **4** (filled). The inset in Fig. 4c shows the low field region 0–4 kOe K^{-1}. Curves show theoretical data for $S = 2/2$ (—·—), 3/2 (—), 4/2 (···), and 5/2 (– – –).

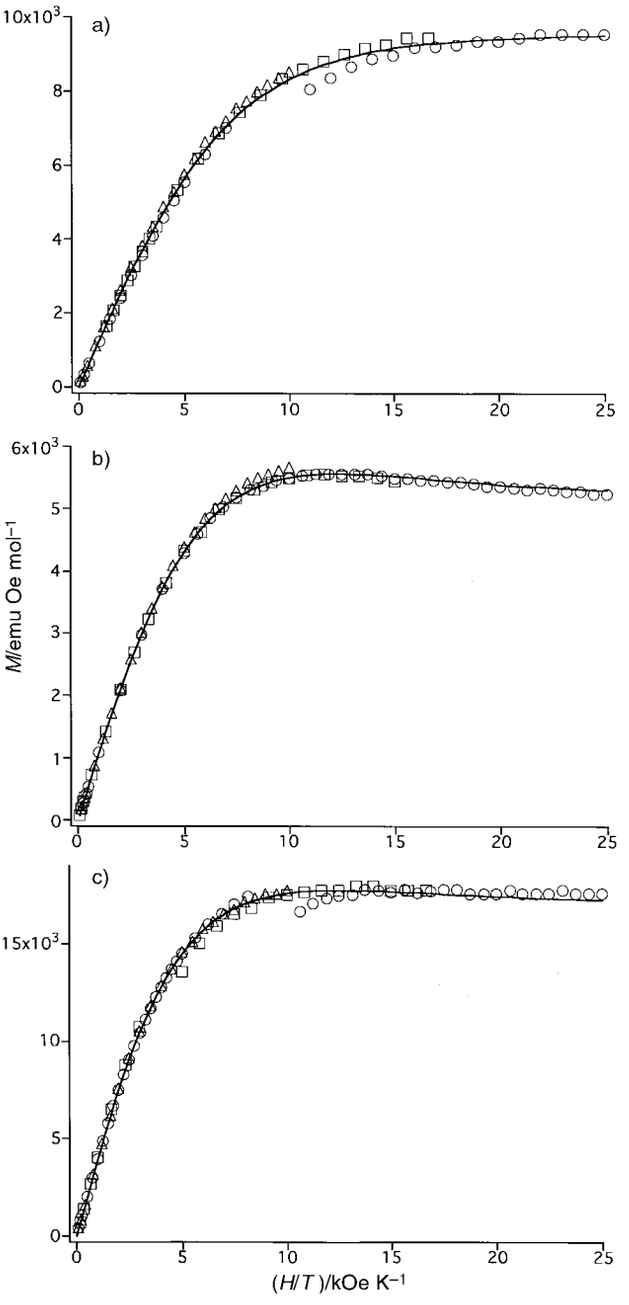

Fig. 5 *M vs.* H/T plots for the complexes of $Cu(hfac)_2$ with (a) **2**, (b) **3** and (c) **4** at 2.0 (○), 3.0 (□), and 5.0 K (△) in frozen MTHF solutions. Theoretical data are shown as solid lines.

UV–Vis spectra before and after SQUID measurements, the degrees of photolysis of **2**, **3**, and **4** were estimated to be 100, 100, and 75%, respectively. These values are close to the photolysis factor ($F = 0.89$, 0.88, and 0.63 for **2c**, **3c**, and **4c**, respectively) obtained by fitting eqn. (1) to the experimental data.

(C)-2 Complexes of Cu(hfac)$_2$ with 2, 3, and 4. Mixed solutions (1.1, 3.5, and 0.5 mM, respectively) of $Cu(hfac)_2$ with **2**, **3**, and **4** in MTHF in ratios of 1 : 1, 2 : 1, and 2 : 1, respectively, were used as the samples. The magnetic measurements were performed under conditions similar to those for the corresponding free ligand.

The *M vs.* H/T plots for the complexes of $Cu(hfac)_2$ with **2**, **3**, and **4** are shown in Fig. 5.

The points where the experimental data deviate from the theoretical curves observed in Fig. 5 are caused by the raw data crossing the zero point of M (from the paramagnetic to the diamagnetic region). The raw data beyond the sensitivity range of the SQUID magnetometer, which were seen as discontinuous data points, were omitted.

The magnetization of the copper complexes before and after irradiation (M_b and M_a, respectively) is expressed as follows:

$$M_b = M_{Cu} + M_{dia} \quad (2)$$

$$M_a = FM_{comp} + (1-F)M_{Cu} + M_{dia} \quad (3)$$

where M_{comp} and M_{Cu} are the magnetizations due to the carbene-Cu complexes and the diazo-copper complexes, respectively, and F is a photolysis factor. The magnetization

(M) due to the species generated by photolysis was obtained as the difference between M_a and M_b: $M = M_a - M_b = F(M_{comp} - M_{Cu})$. The experimental data were analyzed by best-fitting the Brillouin function $B(x)$ as given by eqn. (4):

$$M = M_a - M_b = F(M_{comp} - M_{Cu}) = FNg\mu_B\{SB(x) - B(x')/2\} \quad (4)$$

where $x = gS\mu_B H/(k_B T)$, $x' = g'\mu_B H/(2k_B T)$, and the other symbols have their usual meaning. The g' values for the complexes of Cu(hfac)$_2$ with **2**, **3**, and **4** were 2.16, 2.17, and 2.15, respectively, which were obtained from EPR spectra before irradiation under similar conditions. Eqn. (4) fitted experimental data (M *vs.* H/T) for the 1 : 1 mixture of Cu(hfac)$_2$ and **2** after irradiation for 90 min to give $S = 1.53 \pm 0.01$ and $F = 0.87 \pm 0.01$. Similarly, magnetic field dependences of M for 1 : 2 mixtures of Cu(hfac)$_2$ with **3** and **4** in solutions of MTHF were investigated under similar conditions.

$$M = M_a - M_b = F(M_{comp} - 2M_{Cu}) = FNg\mu_B\{SB(x) - B(x')\} \quad (4')$$

Eqn. (4′) fitted experimental data (M *vs.* H/T) to give $S = 2.14 \pm 0.03$ and 2.86 ± 0.04 and $F = 0.44 \pm 0.01$ and 0.86 ± 0.02 for 2 : 1 mixtures of Cu(hfac)$_2$ with **3** and **4**, respectively. The fitting curves for the complexes of Cu(hfac)$_2$ with **2**, **3**, and **4** are shown in Fig. 5.

From the difference of the absorption (*ca.* 360 nm) due to diazo moieties in the UV–Vis spectra before and after the SQUID measurements, the degrees of photolysis of the complexes of Cu(hfac)$_2$ with **2**, **3**, and **4** were estimated to be 100, 51, and 100%, respectively. These values are close to the photolysis factors ($F = 0.87$, 0.44 and 0.86) obtained by fitting eqn. (4) and (4′) to the experimental data.[17] The obtained S values of 1.53, 2.14, and 2.86 for the complexes of Cu(hfac)$_2$ with **2**, **3**, and **4** are close to the theoretical ones of 1.5, 2.0, and 3.0, respectively. Therefore, this result of the field dependence of M for the complexes of Cu(hfac)$_2$ with **2**, **3**, and **4** suggests that the generated carbene centers interacted with copper(II) ions ferromagnetically to form high-spin complexes with the quartet, quintet and septet ground states, respectively.

Conclusions

The observed UV–Vis and EPR spectra after irradiation of copper(II) complexes in frozen solutions were obviously different from those for metal-free diazo compounds, indicating that the complexes of Cu(hfac)$_2$ coordinated with diazobipyridines were formed in quantitative yields under these frozen solution conditions. In particular, the lack of EPR signals due to free carbenes strongly supported complexation. It became possible to determine the ground-state spin multiplicity of carbene–metal complexes by SQUID measurements before and after irradiation of the diazo–metal precursors under frozen solution conditions. Thus the field dependence of magnetization in solid MTHF solution obviously indicates that the generated carbene interacts ferromagnetically with the copper(II) through the 2,2′-bipyridine ring to produce a high-spin species: quartet, quintet, and septet for [Cu(hfac)$_2$·**2**], [(Cu(hfac)$_2$)$_2$·**3**], and [(Cu(hfac)$_2$)$_2$·**4**], respectively, in the ground state. The sign for exchange coupling between copper and carbene is consistent with the one for [Cu(hfac)$_2$·**1**]; ferromagnetic coupling with $J/k_B = +67$ K. Although the simulation of the EPR spectra for the copper complexes was unsuccessful at this point, the observed EPR and UV–Vis spectra were concluded to be due to the corresponding high-spin species in the ground state. The preparation and investigation of the magnetic properties of 1 : 1 and 2 : 3 complexes of Cu(NO$_3$)$_2$ coordinated with **3** and **4** which are expected to produce super higher-spin species, are in progress.

Experimental

General methods

Infrared spectra were measured on a JASCO FT/IR 420 IR spectrometer. ^{1}H NMR spectra were measured on a JEOL 270 Fourier transform spectrometer using $CDCl_3$ as solvent and referenced to TMS. FAB mass spectra (FAB MS) were recorded on a JEOL JMS-SX102 spectrometer. Melting points were obtained with a MEL-TEMP heating block and are uncorrected. Elemental analyses were performed at the Analytical Center of the Faculty of Science in Kyushu University. Irradiations for UV–Vis and EPR spectroscopic experiments consisted of light of $\lambda > 380$ nm shone through a colored glass filter (Toshiba L-40) from a high-pressure Hg lamp (USHIO; Model UI-501C).

UV–Vis spectra

UV–Vis spectra were recorded on a JASCO V570 spectrometer and a NACC Cryo-system LTS-22X was attached for the low-temperature measurements. The degassed sample solution was placed in a quartz cell of path-length 1 mm.

X-Ray crystal and molecular structural analyses

Diffraction data were collected using MoKα radiation on a Rigaku RAXIS-IV imaging plate area detector system at room temperature for **2** and **4**, and −100 °C for **3** and [Cu(hfac)$_2$·**2**]. The structures for **2**, **3**, **4**, and [Cu(hfac)$_2$·**2**] were solved in space groups $P2_1/n$ (no. 14), $Pbcn$ (no. 60), $Pca2_1$ (no. 29), and $P2_1/c$ (no. 14), respectively, by direct methods[18] and refinement converged using full-matrix least squares methods from the teXsan[19] crystallographic software package (ver. 1.9). All non-hydrogen atoms were refined anisotropically; hydrogen atoms were included at standard positions (C–H 0.96 Å, C–C–H 120°) and refined isotropically using a rigid model.

Crystallographic data and experimental parameters for diazo-bipyridines and their copper complexes are summarized in Table 3. CCDC reference number 1145/265. See http://www.rsc.org/suppdata/jm/b0/b007375j/ for crystallographic files in .cif format.

Magnetic measurements

(A) EPR spectra. EPR spectra were recorded on a Bruker ESP300 X-band (9.4 GHz) spectrometer equipped with a Hewlett Packard 5350B microwave frequency counter. An Air Products LTD-3-110 liquid helium transfer system was attached for the low-temperature measurements. Sample solutions were placed in 5 mm o.d. quartz tubes, degassed by three freeze-and-thaw cycles, and sealed.

(B) SQUID measurements. Magnetic susceptibility data were obtained on a Quantum Design MPMS-5S (0-50 kOe) SQUID magnetometer/susceptometer. Irradiation with light from an argon ion laser (514 nm, 200 mW, Omnichrome 543-200M) and a He–Cd laser (442 nm, 100 mW, Omnichrome 100B-110V) through a flexible optical fiber (Newport F-MBD; 3 m length, 1.0 mm core size, 1.4 mm diameter) which passes through the inside of the SQUID sample holder was performed inside the SQUID sample room of SQUID at 7 K. One end of the optical fiber was located 40 mm above the sample cell (capsule) and the other was attached to a coupler (Body; Newport M-F-916T and lens; M-10X) for the lasers. The bottom part of the capsule (6 mm × 10 mm) without a cap was used as a sample cell. 100 μl of the sample solution (1.1, 3.5 and 0.5 mM for the Cu complexes with **2**, **3**, and **4**, respectively) in MTHF was placed in the cell which was held by a straw.

Table 3 Crystal data and structure refinements for **2**, **3**, **4**, and [Cu(hfac)$_2$·**2**]

	2	**3**	**4**	[Cu(hfac)$_2$·**2**]
Empirical formula	$C_{17}H_{12}N_4$	$C_{21}H_{14}N_6$	$C_{30}H_{22}N_8$	$C_{27}H_{14}N_4O_4F_{12}Cu·C_3H_6O$
Formula weight	272.31	350.38	494.56	808.04
Crystal colour, habit	Red, needles	Orange, plates	Red, plates	Green, needles
Crystal dimensions/mm	0.7 × 0.5 × 0.2	0.1 × 0.1 × 0.02	0.1 × 0.1 × 0.1	0.3 × 0.1 × 0.1
Crystal system	Monoclinic	Orthorhombic	Orthorhombic	Monoclinic
Lattice parameters:				
a/Å	11.518(2)	6.5760(3)	12.5836(2)	15.659(1)
b/Å	6.492(1)	12.5789(7)	7.4541(1)	8.8664(8)
c/Å	18.766(2)	20.624(1)	26.0718(5)	24.206(2)
β/°	97.041(5)			99.801(4)
V/Å^3	1392.7(3)	1706.0(4)	2445.52(7)	3311.7(5)
Space group	$P2_1/n$ (no. 14)	*Pbcn* (no. 60)	$Pca2_1$ (no. 29)	$P2_1/c$ (no. 14)
Z	4	4	4	4
D_{calc}/g cm^{-3}	1.299	1.364	1.343	1.621
No. observations	2517	1204	2480	3987
No. variables	190	125	344	525
Residuals: *R*, *Rw*	0.047; 0.065	0.074; 0.053	0.046; 0.049	0.063; 0.059

Preparation of the 2,2′-bipyridine ligands and the metal complexes

Unless otherwise stated, preparative reactions were carried out under a high-purity dry nitrogen atmosphere. Diethyl ether was distilled from sodium benzophenone ketyl. Bis(hexafluoroacetylacetonato)copper(II), 4-bromo-2,2′-bipyridine,[9] and 4-formyl-4′-methyl-2,2′-bipyridine[20] were prepared and purified by the literature procedures.

4-(α-Hydroxybenzyl)-2,2′-bipyridine 2oh. To a solution of 2.06 g (8.76 mmol) of 4-bromo-2,2′-bipyridine in 120 ml of anhydrous ether were added 14.0 ml (22.4 mmol) of a 1.6 M solution of *n*-butyllithium in *n*-hexane at −78 °C. After stirring for 1 h, 4 ml (39.3 mmol) of benzaldehyde were added dropwise. The reaction mixture was stirred for 1 h at −78 °C. After the usual work-up, crude carbinol **2oh** was chromatographed on silica gel with *n*-hexane–ethyl acetate (1 : 2) to give **2oh** (350 mg, 1.33 mmol) as a white solid in 15.1% yield. Mp 115–116 °C; IR (KBr) 3229 cm^{-1}; ^{1}H NMR ($CDCl_3$, 270 MHz) *δ* 8.55–8.53 (m, 2H), 8.45 (*s*, 1H), 8.31 (d, *J* = 8.0 Hz, 1H), 7.77 (td, *J* = 7.8 and 1.7 Hz, 1H), 7.39–7.36 (m, 2H), 7.33–7.22 (m, 5H), 5.85 (s, 1H), 4.04 (s, 1H); mass spectrum (FAB, *m*-nitrobenzyl alcohol matrix) *m*/*z* 263 ($M^+ + 1$); Anal. Calcd. for $C_{17}H_{14}N_2O$: C, 77.84; H, 5.38; N, 10.64. Found: C, 77.77; H, 5.38; N, 10.59%.

4-Benzoyl-2,2′-bipyridine 2k. To a solution of 0.30 g of the crude carbinol **2oh** in 20 ml of anhydrous $CHCl_3$ were added 1.5 g of freshly prepared MnO_2. The suspension was stirred and refluxed for 1 h and filtered. After filtration, the solvent was evaporated and the crude mixture was chromatographed (silica gel; eluent, *n*-hexane : AcOEt = 1 : 1) to give ketone **2k** as a white solid in 83% yield (0.25 g, 0.96 mmol). Mp 95–96 °C; IR (KBr) 1666 cm^{-1}; ^{1}H NMR ($CDCl_3$, 270 MHz) *δ* 8.85 (dd, *J* = 4.9 and 0.9 Hz, 1H), 8.67–8.64 (m, 2H), 8.44 (ddd, *J* = 8.0, 0.9, and 0.9 Hz, 1H), 7.89–7.80 (m, 3H), 7.64 (tt, *J* = 7.3 and 1.8 Hz, 1H), 7.60 (dd, *J* = 4.9 and 1.6 Hz, 1H), 7.54–7.48 (m, 2H), 7.32 (ddd, *J* = 7.5, 4.8, and 0.9 Hz, 1H); mass spectrum (FAB, *m*-nitrobenzyl alcohol matrix) *m*/*z* 261 ($M^+ + 1$); Anal. Calcd. for $C_{17}H_{12}N_2O$: C, 78.44; H, 4.65; N, 10.76. Found: C, 78.49; H, 4.68; N, 10.72%.

4-(2,2′-Bipyridyl) 4-(2-bromopyridyl) carbinol 3′oh. To a solution of 2.3 g (9.8 mmol) of 4-bromo-2,2′-bipyridine in 150 ml of anhydrous ether were added 13.5 ml (21.5 mmol) of a 1.53 M solution of *n*-butyllithium in *n*-hexane at −78 °C. After stirring for 40 min, a solution of 2.2 g (11.8 mmol) of 2-bromo-4-formylpyridine[21] in 70 ml of anhydrous ether was added dropwise. The reaction mixture was stirred for 30 min at −78 °C and then left overnight after removal of the cooling bath. After the usual work-up, the crude mixture was chromatographed (silica gel; eluent, $CHCl_3$) to give carbinol **3′oh** as a brown solid in 27% yield (0.9 g, 2.6 mmol). Mp 49–51 °C; IR (KBr) 3336 cm^{-1}; ^{1}H NMR ($CDCl_3$, 270 MHz) *δ* 8.49 (dd, *J* = 5.9 and 1.1 Hz, 2H), 8.25 (d, *J* = 7.4 Hz, 1H), 8.16 (d, *J* = 5.1 Hz, 2H), 7.89–7.70 (m, 2H), 7.27–7.22 (m, 1H), 7.19–7.13 (m, 2H), 5.69 (s, 1H); mass spectrum (FAB, *m*-nitrobenzyl alcohol matrix) *m*/*z* 342 ($M^+ + 1$).

4-(2,2′-Bipyridyl) 4-(2-bromopyridyl) ketone 3′k. To a solution of 0.88 g of this crude carbinol **3′oh** in 30 ml of anhydrous $CHCl_3$ were added 2.0 g of freshly prepared MnO_2. The suspension was stirred and refluxed for 2 h and filtered. After filtration, the solvent was evaporated and the crude mixture was chromatographed (Silica gel; eluent, $CHCl_3$) to give ketone **3′k** as a white solid in 71% yield (0.62 g, 1.8 mmol). Mp 142–143 °C; IR (KBr) 1645 cm^{-1}; ^{1}H NMR ($CDCl_3$, 270 MHz) *δ* 8.92 (dd, *J* = 4.9 and 1.1 Hz, 1H), 8.69–8.67 (m, 2H), 8.62 (d, *J* = 5.0 Hz, 1H), 8.49 (m, 1H), 7.90–7.87 (m, 1H), 7.84 (s, 1H), 7.64–7.60 (m, 1H), 7.59 (d, *J* = 1.5 Hz, 1H), 7.39–7.34 (m, 1H); mass spectrum (FAB, *m*-nitrobenzyl alcohol matrix) *m*/*z* 340 ($M^+ + 1$); Anal. Calcd. for $C_{16}H_{11}N_2O_2$: C, 56.49; H, 2.96; N, 12.35. Found: C, 56.40; H, 2.97; N, 12.17%.

Di(4-(2,2′-bipyridyl)oxomethane 3k. A solution of 0.62 g (1.8 mmol) of ketone **3′k**, 0.58 g (2.4 mmol) of 2-trimethylstannylpyridine,[22] and 0.03 g of $Pd(PPh_3)_4$ in 20 ml of anhydrous toluene was refluxed for 6 h. After the usual work-up, the crude mixture was chromatographed (Al_2O_3: activity I; eluents, CH_2Cl_2 : *n*-hexane = 2 : 1) to give ketone **3k** as white solids in 48% yield (0.30 g, 0.86 mmol). Mp 140–142 °C; IR (KBr) 1671 cm^{-1}, ^{1}H NMR ($CDCl_3$, 270 MHz) *δ* 8.92 (dd, *J* = 4.9 and 0.9 Hz, 2H), 8.73 (dd, *J* = 1.6 and 0.9 Hz, 2H), 8.65 (ddd, *J* = 4.8, 1.8, and 1.0 Hz, 2H), 8.47 (d, *J* = 7.5 Hz, 2H), 7.84 (td, *J* = 7.5 and 1.8 Hz, 2H), 7.67 (dd, *J* = 4.9 and 1.6 Hz, 2H), 7.35 (ddd, *J* = 7.5, 4.8, and 1.0 Hz, 2H); mass spectrum (FAB, *m*-nitrobenzyl alcohol matrix) *m*/*z* 339 ($M^+ + 1$); Anal. Calcd. for $C_{21}H_{14}N_4O$: C, 74.54; H, 4.17; N, 16.56. Found: C, 74.59; H, 4.20; N, 16.59%.

1,3-Phenylenebis(4-(4′-methyl-2,2′-bipyridyl)oxomethane) 4k. To a solution of 1.78 g (7.5 mmol) of 1,3-dibromobenzene in 40 ml of anhydrous ether were added 24.6 ml (37.1 mmol) of a 1.51 M solution of *tert*-butyllithium in *n*-pentane at −78 °C. After stirring for 30 min, 3.0 g (15 mmol) of 4-formyl-4′-methyl-2,2′-bipyridine[20] in 30 ml of anhydrous THF were added dropwise. The reaction mixture was stirred for 1 h at −78 °C and then the temperature was raised by the

removal of the cooling bath. After the usual work-up, 4.61 g of crude carbinol **4oh** was obtained as a brown oil. The obtained mixture was used for the oxidation without separation and purification of the carbinol.

To a solution of 4.61 g of this crude carbinol **4oh** in 100 ml of anhydrous $CHCl_3$ were added 14.9 g of freshly prepared MnO_2. The suspension was stirred and refluxed for 3 h and filtered. After filtration, the solvent was evaporated and the crude mixture was chromatographed (Al_2O_3, activity IV; eluent, $CHCl_3$: *n*-hexane = 1 : 1) to give ketone **4k** as a white solid in 28.5% yield (1.01 g, 2.14 mmol). Mp 170–171 °C; IR (KBr) 1670 cm^{-1}; ^1H NMR ($CDCl_3$, 270 MHz) δ 8.74 (dd, J = 4.9 and 0.7 Hz, 2H), 8.69 (m, 2H), 8.53 (d, J = 4.9 Hz, 2H), 8.27 (m, 3H), 8.18 (dd, J = 7.7 and 1.7 Hz, 2H), 7.73 (t, J = 7.7 Hz, 1H), 7.64 (dd, J = 4.9 and 1.7 Hz, 2H), 7.17 (d, J = 4.9 Hz, 2H), 2.46 (s, 6H); mass spectrum (FAB, *m*-nitrobenzyl alcohol matrix) *m/z* 471 ($M^+ + 1$); Anal. Calcd. for $C_{30}H_{22}N_4O_2$: C, 76.58; H, 4.71; N, 11.91. Found: C, 76.57; H, 4.72; N, 11.97%.

General procedure for the preparation of diazo compounds

A solution of 0.40 g (1.52 mmol) of ketone **2k** and 1 ml of anhydrous hydrazine in 2 ml of dimethyl sulfoxide in the presence of hydrazine monohydrochloride (1 g) was heated at 60–80 °C. The cooled reaction mixture was treated with ice-water and the white precipitate was collected and dried under vacuum to give 0.35 g (1.27 mmol) of the corresponding hydrazone in 83% yield. To a solution of 0.35 g (1.27 mmol) of the hydrazone in 10 ml of CH_2Cl_2 was added 1 g of freshly prepared active MnO_2. The mixture was stirred vigorously for 1 h with careful exclusion of light and filtered. The filtrate was concentrated under vacuum to give reddish solids which were recrystallized from suitable solvents.

4-(α-Diazobenzyl)-2,2′-bipyridine 2. Recrystallization from *n*-hexane–ether (1 : 1) gave diazo-bipyridine **2** as red needles. Mp 108 °C (decomp.); IR (KBr disc) $\nu_{C=N_2}$ 2049 cm^{-1}; UV–Vis in MTHF, λ_{max} (log ε): 283 (4.46) and 500 (2.06) nm; ^1H NMR (270 MHz, $CDCl_3$) δ 8.65 (d, J = 4.8 Hz, 1H), 8.54 (d, J = 5.5 Hz, 1H), 8.38 (d, J = 7.9 Hz, 1H), 8.24 (d, J = 2.0 Hz, 1H), 7.81 (dt, J = 5.5 and 1.8 Hz, 1H), 7.50–7.41 (m, 4H), 7.35–7.26 (m, 2H), 7.11 (dd, J = 5.5 and 2.0 Hz, 1H); FAB mass (in NBA matrix), ($M^+ + 1$) 273; Anal. Calcd. for $C_{17}H_{12}N_4$: C, 74.98; H, 4.44; N, 20.57. Found: C, 74.98; H, 4.47; N, 20.53%.

Diazodi{4-(2,2′-bipyridyl)}methane 3. Recrystallization from CH_2Cl_2–ether–MeOH (1 : 1 : 2) gave diazo **3** as orange plates. Mp 165–166 °C (decomp.); IR (KBr disc) $\nu_{C=N_2}$ 2049 cm^{-1}; UV–Vis in MTHF, λ_{max} (log ε): 285 (4.56) and 477 (2.11) nm; ^1H NMR (270 MHz, $CDCl_3$) δ 8.76–8.60 (m, 4H), 8.49–8.39 (m, 4H), 7.89 (dt, J = 7.6 and 1.6 Hz, 2H), 7.39–7.32 (m, 4H); FAB mass (in NBA matrix), ($M^+ + 1$) 351; Anal. Calcd. for $C_{21}H_{14}N_6$: C, 71.99; H, 4.03; N, 23.99. Found: C, 71.86; H, 4.02; N, 23.85%.

1,3-Benzenediyl{4-(4′-methyl-2,2′-bipyridyl)diazomethane} 4. Recrystallization from CH_2Cl_2–*n*-hexane (10 : 1) gave diazo **4** as red plates. Mp 105 °C (decomp.); IR (KBr disc) $\nu_{C=N_2}$ 2049 cm^{-1}; UV–Vis in MTHF, λ_{max} (log ε): 285 (4.91) and 493 (2.38) nm; ^1H NMR (270 MHz, $CDCl_3$) δ 8.52 (d, J = 5.1 Hz, 2H), 8.45 (dd, J = 5.3 and 0.7 Hz, 2H), 8.29 (dd, J = 2.0 and 0.7 Hz, 2H), 8.23–8.22 (m, 2H), 7.54 (t, J = 7.8 Hz, 1H), 7.47 (t, 1.8 Hz, 1H), 7.32 (dd, J = 7.8 and 1.8 Hz, 2H), 7.16 (dd, J = 5.5 and 2.0 Hz, 2H), 7.16–7.13 (m, 2H), 2.44 (s, 6H); FAB mass (in NBA matrix), ($M^+ + 1$) 495; Anal. Calcd. For $C_{30}H_{22}N_8$: C, 72.86; H, 4.48; N, 22.66. Found: C, 72.72; H, 4.45; N, 22.35%.

[Cu(hfac)$_2$·2]. A solution of **2** in acetone–H_2O (5 : 1) was mixed with solutions of Cu(hfac)$_2$ in acetone–H_2O in a molar ratio of 1 : 1 and the mixtures were left in a refrigerator. Single crystals of complexes [Cu(hfac)$_2$·**2**] were obtained as green needles in 17.4% yield. Mp 106–107 °C (decomp.); Anal. Calcd. for $C_{27}H_{14}N_4O_4F_{12}Cu \cdot 0.3C_3H_6O$: C 43.67; H, 2.08; N, 7.30. Found: C, 43.77; H, 2.08; N, 7.33%.

[(Cu(hfac)$_2$)$_2$·3]. The complex was prepared in a manner similar to the procedure for [Cu(hfac)$_2$·**2**] using **3** in a molar ratio of 2 : 1. [(Cu(hfac)$_2$)$_2$·**3**] was obtained as a greenish powder. Mp 122–124 °C (decomp.); Anal. Calcd. for $C_{41}H_{18}N_6O_8F_{24}Cu_2$: C 37.76; H, 1.39; N, 6.44. Found: C, 38.04; H, 1.41; N, 6.31%.

[(Cu(hfac)$_2$)$_2$·4]. The complex was prepared in a manner similar to the procedure for [Cu(hfac)$_2$·**2**] using **4** in a molar ratio of 2 : 1. [(Cu(hfac)$_2$)$_2$·**4**] was obtained as a greenish powder. Mp 120–122 °C (decomp.), Anal. Calcd. for $C_{50}H_{26}N_8O_8F_{24}Cu_2$: C 41.23; H, 1.81; N, 7.73. Found: C, 41.35; H, 1.86; N, 7.61%.

Acknowledgements

This work was supported by a Grant-in-Aid for COE Research "Design and Control of Advanced Molecular Assembly Systems" (#08CE2005) from the Ministry of Education, Science, Sports and Culture, Japan.

References

1 N. Koga and H. Iwamura, *Magnetic Properties of Organic Materials*, ed. P. Lahti, Marcel Dekker, Inc. New York, 1999, ch. 30, p. 629; H. Iwamura and N. Koga, *Pure Appl. Chem.*, 1999, **71**, 231.
2 S. Karasawa, Y. Sano, T. Akita, N. Koga, T. Itoh, H. Iwamura, P. Rabu and M. Drillon, *J. Am. Chem. Soc.*, 1998, **120**, 10080.
3 Y. Sano, M. Tanaka, N. Koga, K. Matsuda, H. Iwamura, P. Rabu and M. Drillon, *J. Am. Chem. Soc.*, 1997, **119**, 8246; N. Koga and H. Iwamura, *Mol. Cryst. Liq. Cryst.*, 1997, **305**, 415; S. Karasawa, M. Tanaka, N. Koga and H. Iwamura, *Chem. Commun.*, 1997, 1359.
4 K. Inoue, T. Hayamizu, H. Iwamura, D. Hashizume and Y. Ohashi, *J. Am. Chem. Soc.*, 1996, **118**, 1803; K. Inoue and H. Iwamura, *J. Am. Chem. Soc.*, 1994, **116**, 3173; A. Caneschi, D. Gatteschi, R. Sessoli and P. Rey, *Acc. Chem. Res.*, 1989, **22**, 392.
5 C. Stroh and R. Ziessel, *Tetrahedron Lett.*, 1999, **40**, 4543; R. Ziessel, G. Ulrich, R. C. Lawson and L. Echegoyen, *J. Mater. Chem.*, 1999, **9**, 1435.
6 C. Kaes, M. W. Hosseini, C. E. F. Rickard, B. W. Skelton and A. H. White, *Angew. Chem., Int. Ed.*, 1998, 37; C. Piguet, G. Bernardinelli and G. Hopfgartner, *Chem. Rev.*, 1997, **98**, 2005; S. Ishiguro, L. Nagy and H. Ohtaki, *Bull. Chem. Soc. Jpn.*, 1987, **60**, 2053; H. Nakai, *Bull. Chem. Soc. Jpn.*, 1980, **53**, 1321.
7 K. Matsuda and H. Iwamura, *J. Am. Chem. Soc.*, 1997, **119**, 7412; K. Matsuda, N. Nakamura, K. Takahashi, K. Inoue, N. Koga and H. Iwamura, *J. Am. Chem. Soc.*, 1995, **117**, 5550.
8 H. Kumada, A. Sakane, N. Koga and H. Iwamura, *J. Chem. Soc., Dalton Trans.*, 2000, 911; A. Sakane, H. Kumada, S. Karasawa, N. Koga and H. Iwamura, *Inorg. Chem.*, 2000, **39**, 2891.
9 J. Sauer, D. K. Heldmann and G. R. Pabst, *Eur. J. Org. Chem.*, 1999, 313.
10 L. L. Merritt Jr. and E. D. Schroeder, *Acta Crystallogr.*, 1956, **9**, 801.
11 A. M. Trozzolo and W. A. Gibbons, *J. Am. Chem. Soc.*, 1967, **89**, 239; W. Sander, G. Bucher and S. Wierlacher, *Chem. Rev.*, 1993, **93**, 1583.
12 S. Cabani, G. Moretti and E. Scrocco, *J. Chem. Soc.*, 1962, 88.
13 C. Murray and C. Wentrup, *J. Am. Chem. Soc.*, 1975, **97**, 7467.
14 N. Koga, Y. Ishimaru and H. Iwamura, *Angew. Chem., Int. Ed. Engl.*, 1996, **35**, 755.
15 S. Murata, T. Sugawara and H. Iwamura, *J. Am. Chem. Soc.*, 1987, **109**, 1266; K. Itoh, *Pure Appl. Chem.*, 1978, **50**, 1251.
16 W. Weltner Jr., *Magnetic Atoms and Molecules*, Van Nostrand Reinhold Co., New York, 1983.
17 Whereas the *F* and *S* values are correlated, the former are more sensitive to the height of the fitted curve and the latter values are sensitive to the curvature. The *F* values obtained by the fitting tend

to be smaller by 10–20% than the degree of photolysis estimated from the UV–Vis absorptions before and after SQUID measurements. The discrepancy between the UV–Vis results and F values might be due to the stability of the generated carbene especially under frozen solution conditions. This is an important problem in this work and is being investigated in detail.

18 SIR92: A. Altomare, M. C. Burla, M. Camalli, M. Cascarano, C. Giacovazzo, A. Guagliardi and G. Polidori, *J. Appl. Cryst.*, 1994, **27**, 435 for **2**, **3**, and [Cu(hfac)$_2$·**2**]; SIR97: A. Altomare, M. C. Burla, M. Camalli, M. Cascarano, C. Giacovazzo, A. Guagliardi, G. Polidori and R. Spagna, *J. Appl. Cryst.*, 1999, **32**, 115 for **4**.

19 Crystal Structure Analysis Package, Molecular Structure Corporation, 1985 & 1992.

20 L. D. Ciana, I. Hamachi and T. J. Meyer, *J. Org. Chem.*, 1989, **54**, 1731.

21 A. Ashimori, T. Ono, T. Uchida, Y. Ohtaki, C. Fukaya, M. Watanabe and K. Yokoyama, *Chem. Pharm. Bull.*, 1990, **38**, 2446.

22 Y. Yamamoto and A. Yanagi, *Chem. Pharm. Bull.*, 1982, **30**, 1731.